DIMENSIONLESS GROUPS FOR MULTIDIMENSIONAL HEAT AND MASS TRANSFER IN ADSORBED NATURAL GAS STORAGE

L. A. Sphaier, lasphaier@mec.uff.br
Laboratório de Mecânica Teórica e Aplicada, Programa de Pós-Graduação em Engenharia Mecânica, Departamento de Engenharia Mecânica, Universidade Federal Fluminense

Abstract. *This paper provides a new methodology for analyzing heat and mass transfer in gas storage via adsorption. The foundation behind the proposed methodology comprises a set of physically meaningful dimensionless groups. A discussion regarding the development of such groups is herein presented, providing a fully normalized multidimensional formulation for describing the transport mechanisms involved in adsorbed gas storage. After such presentation, data from previous literature studies associated with the problem of adsorbed natural gas storage are employed for determining realistic values for the developed parameters. Then, a one-dimensional test-case problem is selected for illustrating the application of the dimensionless formulation for simulating the operation of adsorbed gas reservoirs. The test problem is focused on analyzing an adsorbed gas discharge operation. This problem is numerically solved, and the solution is verified against previously published literature data. The presented results demonstrate how a higher heat of sorption values lead to reduced discharge capacities.*

Keywords: *Natural Gas, Gas Storage, Adsorption, Dimensional Analysis*

1. NOMENCLATURE

Bi	Biot number
c_p	constant pressure specific heat
c^*_{lg}	liquid-to-gas specific heat ratio
C^*	thermal capacity ratio
Fo	Fourier number
h	heat transfer coefficient
i	specific enthalpy
$\boldsymbol{j}''$	mass flux vector
i_{sor}	heat of sorption
k	thermal conductivity
L	diffusion length
m	mass
$\dot{m}$	mass flow rate
$\dot{m}''$	mass flux
M^*_g	maximum compressed gas fraction
M^*_l	maximum adsorbed gas fraction
$\hat{\boldsymbol{n}}$	unit normal vector
p	pressure
$\dot{\boldsymbol{q}}''$	heat flux vector
r	radial coordinate
R	gas constant
t	time
t_f	operation time
T	temperature
$\mathcal{V}$	reservoir volume

Greek Symbols

α	thermal diffusivity
γ	generalized boundary condition parameter
δ_w	reservoir wall thickness
ω	thermodynamic ratio
ρ	specific mass or concentration
σ	coefficient in Darcy equation
ϵ	porosity

Subscripts and Superscripts

$*$	dimensionless quantity
b	porous adsorbent bed
e	effective or apparent
g	gaseous phase
in	inlet/outlet
l	adsorbed (liquid) phase
s	solid phase
w	reservoir wall

2. INTRODUCTION

The constantly growing worldwide demand for gaseous fuels such as natural gas and hydrogen has been motivating the development of efficient gas storage and transportation technologies. Currently, there are two main gas storage methods: compressed gas and liquified gas. Although these storage modes are well established, there are inherent drawbacks. Compressed gas has the disadvantage of working at high pressures, which require heavy reservoirs for transportation and high compression costs. On the other hand, and liquified gas needs cryogenic temperatures and specialized equipment for re-gasification. In this scenario, a relatively new technology comes as a promising alternative: adsorbed gas. This alternative relies on loading the gas into porous sorbent materials and, while compared to the other alternatives, has the advantages of employing lower pressures and requiring no need for extreme temperature reductions. In order to establish adsorbed gas as a commercially viable alternative, it is necessary that it be competitive with the currently available storage modes. However, this can only happen if an appropriate thermal design is achieved, since the sorption effect generates unwanted heating (and cooling) that significantly degrades storage and recovery capabilities. Because of this, a proper understanding of the heat and mass transfer mechanisms that occur within adsorbed gas reservoirs is required. As a result, a number of studies that consider the physical and mathematical modeling of the problem have been carried-out (Barbosa Mota, Rodrigues et al., 1997; Vasiliev, Kanonchik et al., 2000; Bastos-Neto, Torres et al., 2005; Walton and LeVan, 2006; Hirata, Couto et al., 2009; Santos, Marcondes et al., 2009).

In spite of the relevance of the previously proposed formulations, the vast majority of them are apparently limited with respect to the normalization of the problem. Recently, a new lumped formulation was proposed in (da Silva and Sphaier, 2010). The employed model, despite its simplicity, was developed in a fully dimensionless framework. Its development introduced a set of significant dimensionless groups associated with the problem of adsorbed natural gas storage. Nevertheless, since the type of formulation used in that study cannot consider spatial gradients, no dimensionless groups associated with local transport phenomena were obtained. This papers extends the ideas developed in (da Silva and Sphaier, 2010), presenting a set of dimensionless groups valid for multidimensional formulations for heat and mass transfer in adsorbed gas storage. These groups are employed for producing a normalized formulation for describing adsorbed gas storage operations. This formulation then is numerically solved and validated against previously published results. Finally, results of a one-dimensional test-case problem related to gas discharge at a constant mass flow rate are presented.

3. PROBLEM FORMULATION

The problem of gas storage via adsorption involves the transport of heat and mass within a reservoir that is filled with a porous adsorbent. Although differences in formulations may be found among previous investigations, a common representation of the problem, arising from considering usual simplifying assumptions (Barbosa Mota, Rodrigues et al., 1997; Vasiliev, Kanonchik et al., 2000; Bastos-Neto, Torres et al., 2005; Hirata, Couto et al., 2009), is given by the following transport equations:

$$\epsilon \frac{\partial \rho_g}{\partial t} + \frac{\partial \rho_l}{\partial t} = -\nabla \cdot \boldsymbol{j}_g'', \tag{1}$$

$$\rho_e \, c_e \frac{\partial T}{\partial t} + c_{p_g} \boldsymbol{j}_g'' \cdot (\nabla T) = -\nabla \cdot \dot{\boldsymbol{q}}'' + i_{sor} \frac{\partial \rho_l}{\partial t} + \epsilon \frac{\partial p}{\partial t}, \tag{2}$$

in which the product $\rho_e \, c_e$ is the effective thermal capacity and i_{sor} is the differential heat of sorption, in which:

$$\rho_e \, c_e = (\rho_s \, c_s + \rho_l \, c_l) + \rho_g \, c_{p_g} \, \epsilon. \tag{3}$$

These densities (or concentrations) are expressed in terms of temperature and pressure by introducing a equation of state and an adsorption isotherm. These are written in a general form, as

$$\rho_g \,=\, \rho_g(T,p), \qquad\qquad \rho_l \,=\, \rho_l(T,p), \tag{4}$$

in which the functional form will depend on the selected adsorbent and adsorbate.

The gas-phase mass flux can be written using a generalized Darcy's Law and the heat flux is written using Fourier's Law

$$\boldsymbol{j}''_g \,=\, -\,\rho_g\,\sigma\,\nabla p, \qquad\qquad \dot{\boldsymbol{q}}'' \,=\, -k_e\,\nabla T, \tag{5}$$

where the coefficient σ may depend on the pressure gradient and k_e is the effective thermal conductivity of the porous medium.

In this paper, a simplified version of the problem is considered, in which the reservoir wall thermal capacity is considered negligible compared to the capacity of the adsorbent material. Denoting $\mathcal{S}_i$ as the inlet/outlet surface and $\mathcal{S}_e$ as the remaining surface, the boundary conditions are given by:

$$-\boldsymbol{j}''_g\cdot\hat{\boldsymbol{n}} \,=\, \dot{m}''_{in}, \qquad \text{and} \qquad -\,\dot{\boldsymbol{q}}''\cdot\hat{\boldsymbol{n}} \,=\, 0, \qquad \boldsymbol{r} \,\in\, \mathcal{S}_i, \tag{6}$$

$$\boldsymbol{j}''_g\cdot\hat{\boldsymbol{n}} \,=\, 0, \qquad \text{and} \qquad \dot{\boldsymbol{q}}''\cdot\hat{\boldsymbol{n}} \,=\, h\,(T-T_0) \,+\, \rho_w\,c_w\,\delta_w\,\frac{\partial T}{\partial t}, \qquad \boldsymbol{r} \,\in\, \mathcal{S}_e, \tag{7}$$

where $\dot{m}''_{in}$ is the inlet mass flux (normal component).

The initial conditions for the following problem are given in terms of pressure and temperature:

$$p(t=0) \,=\, p_0, \qquad\qquad T(t=0) \,=\, T_0. \tag{8}$$

4. Development of dimensionless groups

Assuming that both charge and discharge processes start from an initial state that is in equilibrium with the surroundings, the maximum and minimum values of gas and adsorbed phase concentrations are given by:

$$\rho_{g,\max} \,=\, \rho_g(p_{\max},T_0), \qquad \rho_{g,\min} \,=\, \rho_g(p_{\min},T_0), \tag{9}$$

$$\rho_{l,\max} \,=\, \rho_l(p_{\max},T_0), \qquad \rho_{l,\min} \,=\, \rho_l(p_{\min},T_0). \tag{10}$$

Based on the minimum and maximum values for ρ_g and ρ_l, one defines the following differences:

$$\Delta\rho_g \,=\, \rho_{g,\max} - \rho_{g,\min}, \qquad \Delta\rho_l \,=\, \rho_{l,\max} - \rho_{l,\min}, \tag{11}$$

representing the maximum changes in these concentrations.

The first dimensionless groups represent the fractions of gas that can be stored in compressed form and in adsorbed form, being respectively defined as

$$\mathrm{M}^*_g \,=\, \frac{\Delta\rho_g\,\epsilon\,\mathcal{V}}{\Delta m_{\max}}, \qquad \mathrm{M}^*_l \,=\, \frac{\Delta\rho_l\,\mathcal{V}}{\Delta m_{\max}}, \qquad \text{where} \qquad \Delta m_{\max} \,=\, (\Delta\rho_g\,\epsilon \,+\, \Delta\rho_l)\,\mathcal{V}. \tag{12}$$

The next parameters comprise thermal capacity ratios between different capacities and that of the amount of gas charged (or discharged) under ideal (isothermal) conditions. In this context, the thermal capacity ratios are respectively defined as:

$$\mathrm{C}^*_s \,=\, \frac{c_s\,\rho_b\,\mathcal{V}}{c_{p_g}\,\Delta m_{\max}}, \quad \mathrm{C}^*_w \,=\, \frac{m_w\,c_w}{c_{p_g}\,\Delta m_{\max}}\,\frac{\mathcal{V}}{\mathcal{V}_w}\,\frac{\delta_w}{L}, \quad \mathrm{C}^*_{\min} \,=\, \frac{\left(\epsilon\,c_{p_g}\,\rho_{g,\min} + c_l\,\rho_{l,\min}\right)\mathcal{V}}{c_{p_g}\,\Delta m_{\max}}. \tag{13}$$

Fourier and Biot numbers are defined as

$$\mathrm{Fo} \,=\, \frac{\alpha_b \, t_f}{L^2}, \quad \text{with} \quad \alpha_b \,=\, \frac{k_b}{\rho_b \, c_s}, \qquad\qquad \mathrm{Bi} \,=\, \frac{h \, L}{k_b}, \tag{14}$$

where k_b is the bed conductivity. Three other parameters is the thermodynamic ratio ω, the dimensionless heat of sorption, and the liquid-to-gas specific heat ratio:

$$\omega \,=\, \frac{p_{\max} - p_{\min}}{\Delta\rho_g \, c_{p_g} \, T_0}, \qquad i^*_{sor} \,=\, \frac{i_{sor}}{T_0 \, c_{p_g}}, \qquad c^*_{lg} \,=\, \frac{c_l}{c_{p_g}}. \tag{15}$$

4.1 Dimensionless variables

The dependent and independent variables are normalized by introducing the following dimensionless forms:

$$t^* \,=\, \frac{t}{t_f}, \quad T^* \,=\, \frac{T}{T_0}, \quad p^* \,=\, \frac{p - p_{\min}}{p_{\max} - p_{\min}}, \quad \rho^*_g \,=\, \frac{\rho_g - \rho_{g,\min}}{\Delta\rho_g}, \quad \rho^*_l \,=\, \frac{\rho_l - \rho_{l,\min}}{\Delta\rho_l}, \tag{16}$$

The dimensionless nabla operator is defined as

$$\nabla^* \,=\, L \, \nabla, \tag{17}$$

and dimensionless versions of the mass flux vector and mass influx, and the total mass stored in the reservoir are respectively defined as:

$$\boldsymbol{j}^* \,=\, \frac{\boldsymbol{j}'' \, t_f}{\Delta m_{\max} \, L/\mathcal{V}}, \qquad j^*_{in} \,=\, \frac{\dot{m}''_{in} \, t_f}{\Delta m_{\max} \, L/\mathcal{V}}, \qquad m^* \,=\, \frac{m_{\text{real}}}{\Delta m_{\max}}. \tag{18}$$

In order to facilitate notation it is also convenient to write the heat conduction in terms of a dimensionless heat flux vector. Using the dimensionless variables, the dimensionless mass flux and heat flux vectors are written as:

$$\boldsymbol{j}^* \,=\, -\mathrm{M}^*_g \, (\rho^*_g + \rho^*_{g,\min}) \, \sigma^* \, \nabla^* p^*, \qquad \boldsymbol{q}^* \,=\, -k^*_e \, \nabla^* T^*, \tag{19}$$

where

$$\sigma^* \,=\, \sigma \, \frac{\Delta p \, t_f}{L^2}, \qquad \rho^*_{g,\min} \,=\, \frac{\rho_{g,\min}}{\Delta\rho_g}. \qquad k^*_e \,=\, \frac{k_e}{k_b}, \tag{20}$$

4.2 Dimensionless multidimensional formulation

Using the dimensionless variables a normalized version of the formulation is obtained:

$$\mathrm{M}^*_g \, \frac{\partial \rho^*_g}{\partial t^*} \,+\, \mathrm{M}^*_l \, \frac{\partial \rho^*_l}{\partial t^*} \,=\, -\,\nabla^* \cdot \boldsymbol{j}^*_g, \tag{21}$$

$$\left(\mathrm{M}^*_g \, \rho^*_g + c^*_{lg} \, \mathrm{M}^*_l \, \rho^*_l + \mathrm{C}^*_s + \mathrm{C}^*_{\min}\right) \, \frac{\partial T^*}{\partial t^*} \,+\, \boldsymbol{j}^*_g \cdot (\nabla^* T^*) \,=$$
$$\,=\, -\mathrm{Fo} \, \mathrm{C}^*_s \, \nabla^* \cdot \boldsymbol{q}^* \,+\, \mathrm{M}^*_l \, i^*_{sor} \, \frac{\partial \rho^*_l}{\partial t^*} \,+\, \mathrm{M}^*_g \, \omega \, \frac{\partial p^*}{\partial t^*}, \tag{22}$$

The dimensionless boundary and initial conditions are given by:

$$\boldsymbol{j}^*_g \cdot \hat{\boldsymbol{n}} \,=\, 0 \qquad \text{and} \qquad -\, k^*_e \, (\nabla^* T^*) \cdot \hat{\boldsymbol{n}} \,=\, \mathrm{Bi} \, (T^* - 1) \,+\, \frac{\mathrm{C}^*_w}{\mathrm{C}^*_s} \, \frac{1}{\mathrm{Fo}} \, \frac{\partial T^*}{\partial t^*}, \qquad \text{at} \quad \mathcal{S}_e \tag{23}$$

$$\boldsymbol{j}^*_g \cdot \hat{\boldsymbol{n}} \,=\, j^*_{in} \qquad \text{and} \qquad -\, k^*_e \, (\nabla^* T^*) \cdot \hat{\boldsymbol{n}} \,=\, 0, \qquad \text{at} \quad \mathcal{S}_i \tag{24}$$

$$p^*(t^* = 0) \,=\, p^*_0 \qquad \text{and} \qquad T^*(t^* = 0) \,=\, 1, \tag{25}$$

in which $p_0^* = 1$ for discharge and $p_0^* = 0$ for charge. By observing the resulting normalized formulation, one clearly notices how the introduction of physically meaningful dimensionless groups into the problem facilitates the analysis. Although the employed dimensionless parameters were introduced with no rigorous presentation, a thorough derivation of dimensionless groups was recently presented in (Sacsa Diaz and Sphaier, 2010).

4.3 Values for dimensionless parameters

In order to establish realistic values for the obtained dimensionless parameters, data used in previous studies were employed for calculating numerical values. Since most surveyed literature studies focus on methane (or natural gas) applications, values particular to these types of applications are presented. Data from different articles were selected, and the resulting values for the dimensionless parameters are presented in table 1. As can be seen, some parameters present a wide range of val-

Table 1. Calculated dimensionless groups values.

Source	M_l^*	C_s^*	$\mathrm{C}_{\min}^*$	C_w^*	Fo	Bi	i_{sor}^*
Barbosa Mota, Rodrigues et al. (1997)	0.68	2.02	0.16	5.11	3.56	0.24	1.58
Bastos-Neto, Torres et al. (2005)	0.58	4.05	0.12	2.75	1.22	8.51	1.33
Basumatary, Dutta et al. (2005)	0.69	2.29	0.14	9.65	0.01	146.	1.65
Chang and Talu (1996)	0.84	5.81	0.38	5.73	0.49	1.04	1.60
Hirata, Couto et al. (2009)	0.66	2.13	0.15	4.64	1.65	0.47	1.53

ues, such as the Fourier and Biot numbers, sometimes varying over an order of magnitude. This is expected, since these parameters are based on the process time (Fo), which can vary significantly depending on the type of process (charge or discharge), and the heat transfer coefficient (Bi), which can assume very different values according to the applied heating (or cooling) rate. The remaining parameters present a smaller variation throughout the analyzed studies. The parameter that presents the smallest variation is the dimensionless heat of sorption. Nevertheless, one should keep in mind that all of the analyzed studies are related to natural gas components being adsorbed on activated carbon. Since the heat of sorption can depend on the sorbate-sorbent pair, i_{sor}^* could present very different values for other combinations of gases and adsorbents.

5. Test-case

After the presentation of the dimensionless groups and resulting normalized formulation, simulation results of a test-case were calculated for illustrating the effect of the dimensionless parameters on the operation of an adsorbed gas reservoir. The simple test-case of slow discharge at a constant mass flow rate from a long cylindrical reservoir was considered. Using the dimensionless parameters and normalization methodology herein described the problem is written as

$$\mathrm{M}_g^* \frac{\partial \rho_g^*}{\partial t^*} + \mathrm{M}_l^* \frac{\partial \rho_l^*}{\partial t^*} = -\frac{1}{r^* + r_{in}^*} \frac{\partial}{\partial r^*} \left((r^* + r_{in}^*)\, j_{g,r}^* \right), \tag{26}$$

$$\left(\mathrm{M}_g^*\, \rho_g^* + c_p^*\, \mathrm{M}_l^*\, \rho_l^* + \mathrm{C}^* \right) \frac{\partial T^*}{\partial t^*} + j_{g,r}^* \frac{\partial T^*}{\partial r^*} = \\ = -\mathrm{C}_s^*\, \mathrm{Fo}\, \frac{1}{r^* + r_{in}^*} \frac{\partial}{\partial r^*} \Big((r^* + r_{in}^*)\, q_r^* \Big) + \mathrm{M}_l^*\, i_{sor}^* \frac{\partial \rho_l^*}{\partial t^*} + \mathrm{M}_g^*\, \omega \frac{\partial p^*}{\partial t^*}, \tag{27}$$

where the heat and mass fluxes are given by:

$$j^*_{g,r} \;=\; -\mathrm{M}^*_g\,(\rho^*_g + \rho^*_{g,\min})\,\sigma^*\,\frac{\partial p^*}{\partial r^*}, \qquad\qquad q^*_r \;=\; -k^*_e\,\frac{\partial T^*}{\partial r^*}, \tag{28}$$

and r^* and r^*_{in} are defined as

$$r^* \;=\; \frac{r - r_{in}}{r_{ex} - r_{in}}, \qquad\qquad r^*_{in} \;=\; \frac{r_{in}}{r_{ex} - r_{in}}. \tag{29}$$

The boundary conditions are given by:

$$j^*_{g,r} \;=\; 0, \qquad \text{at} \qquad r^* = 1, \tag{30}$$

$$-k^*_e\,\frac{\partial T^*}{\partial r^*} \;=\; \mathrm{Bi}\,(T^* - 1) \;+\; \frac{\mathrm{C}^*_w}{\mathrm{C}^*_s}\,\frac{1}{\mathrm{Fo}}\,\frac{\partial T^*}{\partial t^*}, \qquad \text{at} \qquad r^* = 1, \tag{31}$$

$$j^*_{g,r} \;=\; j^*_{in}, \qquad \text{and} \qquad k^*_e\,\frac{\partial T^*}{\partial r^*} \;=\; 0, \qquad \text{at} \qquad r^* = 0, \tag{32}$$

in which, since a discharge operation is considered, $j^*_{in} < 0$.

In the previously presented forms, the proposed formulations have four unknowns (ρ^*_g, ρ^*_l, T^* and p^*) and only two equations. Nevertheless, this is naturally overcome by introducing an equation of state for ρ_g and an adsorption equilibrium correlation (or adsorption isotherm) for ρ_l, which are chosen as:

$$\rho_g \;=\; \rho_g(T, p) \;=\; \frac{p}{R\,T}, \qquad\qquad \frac{\rho_l}{\rho_b} \;=\; q_m\,\frac{b\,p}{1 + b\,p}, \tag{33}$$

in which

$$q_m = 5.592 \times 10^4\,T^{-2.3}, \qquad\qquad b = 1.0863 \times 10^{-7}\exp(806/T). \tag{34}$$

6. RESULTS AND DISCUSSION

The first simulation results are carried-out as a verification of the adopted model, normalization scheme, and, particularly, of the numerical solution implementation. The recent results presented by Hirata, Couto et al. (2009) were selected for comparison purposes. One should mention that the results presented in that study consider a uniform pressure distribution, which leads to a simpler formulation with $p = p(t)$ only. In contrast, the solution implemented in this work allows the pressure to vary spatially, as described by the model equations. In spite of these differences, since a slow discharge situation is considered, the calculated pressure distribution should present small gradients, and therefore both formulations should lead to equivalent results. The numerical solution itself was calculated using the Finite Volumes Method combined to the Numerical Method of Lines. The solution algorithm is based on the scheme described in (Sphaier and Worek, 2008).

Since a slightly different mathematical model was used in (Hirata, Couto et al., 2009), a few adjustments were required to guarantee that the involved physics were unnaltered. First, the value of σ^* was calculated from an average using the data in (Barbosa Mota, Rodrigues et al., 1997), and the value of $\dot{m}^*_{in}$ (invariable with time) was calculated to ensure that the depletion pressure was reached at the end of the process time (that is $p^* = 0$ at $t^* = 1$). Finally, since the solution in (Hirata, Couto et al., 2009) was calculated for a solid cylinder, the inner radius was set to a small value ($r^*_{in} = 10^{-6}$). The values for the dimensionless parameters used in the verification can be found at the end of table 1.

Figure 1 displays comparison results between the calculated average pressure and the pressure distribution obtained from (Hirata, Couto et al., 2009). As can be seen, there is perfect agreement

between the results. Next, figure 2 presents a comparison of spatial temperature distribution at various instants. The presented curves are equally separated in time and the last one corresponds to the end of the discharge process ($t^* = 1$). The initial condition is simply $T = T_0 = 293$ K and needs not be displayed. By observing the results one notices very good agreement between the different data. Minor discrepancies are seen; nevertheless, these are prone to occur since the model equations used in the current study are slightly different than the simpler version used in (Hirata, Couto et al., 2009).

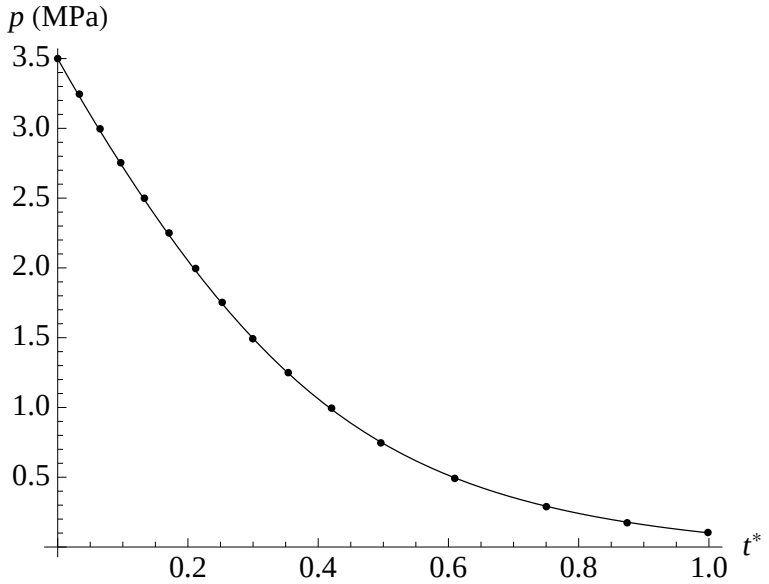

Figure 1. Verification results: average pressure history. The points represent data from Hirata, Couto et al. (2009)

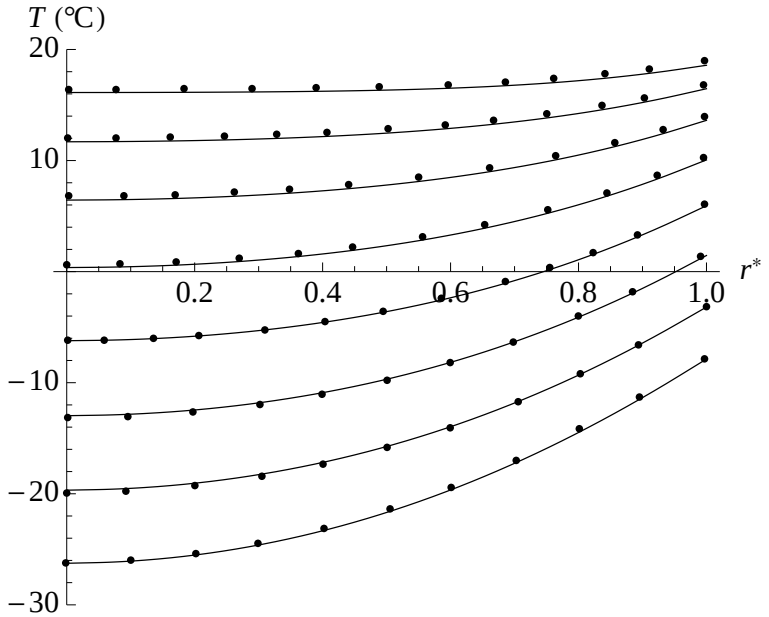

Figure 2. Verification results: temperature distributions at $t^* = 1/8, 1/4, 3/8, 1/2, 5/8, 3/4, 7/8$ and 1 (the temperature monotonically decreases with t^*). The points represent data from Hirata, Couto et al. (2009).

After the previous verification results, simulation results for the test-case problem are carried-

out for illustrating the effect of varying the dimensionless parameters on the adsorbed gas reservoir operation. As previously done, a methane discharge process at constant mass flow rate is analyzed. The data used in these simulations are displayed in table 2.

Table 2. Input data used in test-case simulations

ambient temperature, T_0	293 K
depletion pressure, $p_{\min}$	0.1 MPa
initial pressure, $p_{\max}$	3.5 MPa
specific heat ratio, c^*_{lg}	1
thermal conductivity variation parameter, k^*_e	1
adsorbed gas fraction, M^*_l	0.7
adsorbent thermal capacity ratio, C^*_s	2.0
minimum thermal capacity ratio, $\mathrm{C}^*_{\min}$	0.15
wall thermal capacity ratio, C^*_w	5.0
dimensionless heat of sorption, i^*_{sor}	1.5
dimensionless coefficient in Darcy equation, σ^*	1×10^{10}

Since the important dependent variable for this discharge process is the amount of gas recovered, the subsequent analyses are based on evaluating variations in this quantity, defined in dimensionless form as:

$$\dot{m}^*_{rec} = -\int_0^1 \dot{m}^*_{in}\,\mathrm{d}t^*. \tag{35}$$

Naturally, since $\dot{m}^*_{in}$ is constant the previous relation simply yields $\dot{m}^*_{rec} = |\dot{m}^*_{in}|$. Also, $\dot{m}^*_{rec}$ is equal to unity for an isothermal process. Naturally, for non-isothermal operation, a smaller value is obtained. As a result, the quantity $\dot{m}^*_{rec}$ works as a performance measure of the discharge process. Besides focusing on $\dot{m}^*_{rec}$, as the heat transfer to the surroundings plays an important role in the performance of adsorbed gas reservoirs, all results are plotted against the Biot number Bi.

Figure 3 shows the variation in recovered gas with Bi for different values of the Fourier number. As one can observe, less gas is recovered for smaller values of Bi and Fo. The lower Biot number limit approaches thermal insulation, and hence represents the worse condition, since nearly no heat is exchanged with the surroundings. At the other limit, one notices that increasing the Biot number indefinitely has no advantage since the amount of gas recovered tends to a constant value for $\mathrm{Bi} > 100$ (and lower for the higher values of Fo). By observing the variations in $\dot{m}^*_{rec}$ with the Fourier number, it is clear that higher Fo values lead to better performance. Higher Fourier values can generally be obtained for longer discharge processes, thereby indicating that slower processes can lead to more efficient gas recovery.

Next, figure 4 presents the variation in the amount of gas recovered, again with Bi and Fo, however, for a heat of sorption value twice as in the previous cases. As can be seen, increasing the heat of sorption clearly reduces the amount of gas that can be recovered.

The results presented in this section give a good initial picture of how some of the dimensionless parameters can influence discharge operations in adsorbed gas reservoirs. Qualitatively speaking, similar observations should be seen for charge operations. Nonetheless, most important than these observations is the fact that, with the proposed dimensionless groups methodology, one can analyze adsorbed gas storage problems much more efficiently.

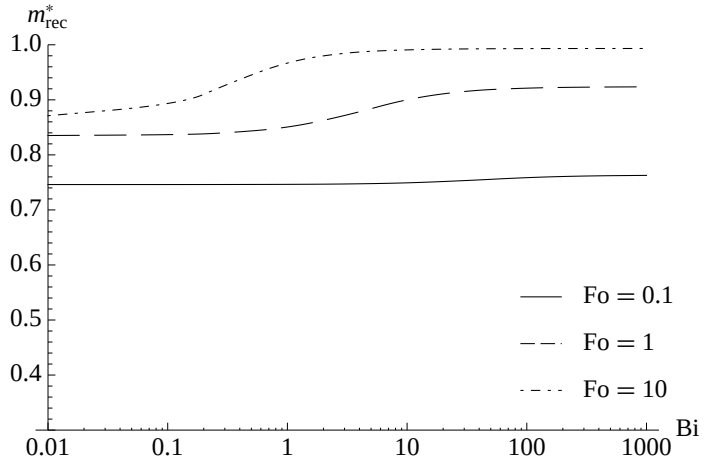

Figure 3. Variation in recovered gas with Bi for $\mathrm{C}^*_s = 2$ and $i^*_{sor} = 1.5$.

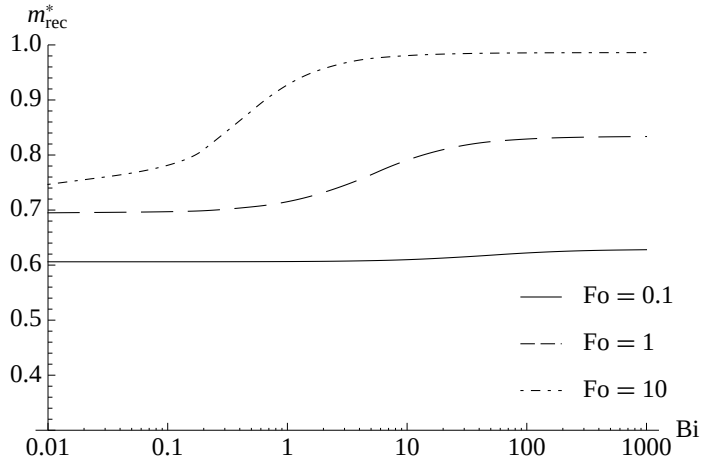

Figure 4. Variation in recovered gas with Bi for $\mathrm{C}^*_s = 2$ and $i^*_{sor} = 3$.

7. Conclusions

This paper introduced a method for analyzing the heat and mass transfer phenomena associated with gas storage operations in adsorbent materials. This advancement was achieved through the development of dimensionless groups associated with the energy and mass transport mechanisms involved in the considered problem. Some of the resulting parameters are traditionally known forms, such as Biot and Fourier numbers, and others are somewhat new to the literature, but most importantly, all of them have a physical meaning. This greatly facilitates analysis and simulation, since a better understanding of the transport phenomena is achieved and a reduced number of parameters is required to characterize the considered problem. The main parameters are: the overall thermal capacity ratio C^*, the adsorbed gas fraction (M^*_l), the dimensionless heat of sorption (i^*_{sor}), and Fourier and Biot numbers. A capacity ratio associated with thermal storage in the reservoir wall was also introduced (C^*_w), as well as a parameter associated with the Darcy flow in the porous medium (σ^*). Finally, two other parameters solely related to the stored gas properties were employed: the thermodynamic ratio ω (associated with compression) and the liquid-to-gas specific heat ratio c^*_{lg}; although these are in fact part of the independent dimensionless parameters, they will only vary if different stored substances are compared. After the presentation of the dimensionless groups, data from different studies were collected for determining realistic values for these groups in natural gas storage applications. The

results indicated that some parameters (such as the Fourier and Biot numbers) can have a greater range of values than the others.

After introducing the dimensionless groups and normalization, a multidimensional heat and mass transfer formulation was obtained. Simulation results from this model were compared with those of a previous study, verifying the model and numerical implementation. After this verification, in order to illustrate the influence of the dimensionless parameters on the behavior of charge operations, simulation results for a test-case was carried-out. The results demonstrated that higher values of Fo and Bi, will generally lead to better performance, since the disadvantageous thermal effect is diminished. In spite of the importance of these demonstrations, they are still preliminary, and more rigorous investigations regarding the effect of the presented groups in adsorbed gas storage operations — including both charge and discharge — should be carried-out.

8. ACKNOWLEDGEMENTS

The authors would like to acknowledge the financial support provided by, CNPq, FAPERJ, and Universidade Federal Fluminense.

REFERENCES

Barbosa Mota, J.P., Rodrigues, A.E., Saatdjian, E., and Tondeur, D., 1997, "Dynamics of natural gas adsorption storage system employing activated carbon", Carbon, vol. 35, no. 9, pp. 1259–1270.

Bastos-Neto, M., Torres, A.E.B., Azevedo, D.C.S., and Jr., C.L.C., 2005, "A theoretical and experimental study of charge and discharge cycles in a storage vessel for adsorbed natural gas", Adsorption, vol. 11, pp. 147–157.

Basumatary, R., Dutta, P., Prasad, M., and Srinivasan, K., 2005, "Thermal modeling of activated carbon based adsorptive natural gas storage system", Carbon, vol. 43, no. 3, pp. 541–549.

Chang, K.J. and Talu, O., 1996, "Behavior and performance of adsorptive natural gas storage cylinders during discharge", Applied Thermal Engineering, vol. 16, no. 5, pp. 359–374.

da Silva, M.J.M. and Sphaier, L.A., 2010, "Dimensionless lumped formulation for performance assesment of adsorbed natural gas storage", Applied Energy, vol. 87, no. 5, pp. 1572–1580.

Hirata, S.C., Couto, P., Larac, L.G., and Cotta, R.M., 2009, "Modeling and hybrid simulation of slow discharge process of adsorbed methane tanks", International Journal of Thermal Sciences, vol. 48, no. 6, pp. 1176–1183.

Sacsa Diaz, R.P. and Sphaier, L.A., 2010, "Development of dimensionless groups for heat and mass transfer in adsorbed gas storage", International Journal of Thermal Sciences, vol. accepted for publication.

Santos, J.C., Marcondes, F., and Gurgel, J.M., 2009, "Performance analysis of a new tank configuration applied to the natural gas storage systems by adsorption", Applied Thermal Engineering, vol. 29, no. 11–12, pp. 2365–2372.

Sphaier, L.A. and Worek, W.M., 2008, "Numerical solution of periodic heat and mass transfer with adsorption in regenerators: Analysis and optimization", Numerical Heat Transfer – Part A, vol. 53, no. 11, pp. 1133–1155.

Vasiliev, L.L., Kanonchik, L., Mishkinis, D., and Rabetsky, M., 2000, "Adsorbed natural gas storage and transportation vessels", International Journal of Thermal Sciences, vol. 39, pp. 1047–1055.

Walton, K.S. and LeVan, M.D., 2006, "Natural gas storage cycles: Influence of nonisothermal effects and heavy alkanes", Adsorption, vol. 12, no. 3, pp. 227–235.

9. RESPONSIBILITY NOTICE

The authors are the only responsible for the printed material included in this paper.